Universiteit
Leiden
The Netherlands

Identification of novel targets in prostate cancer progression

Ghotra, V.P.S.

Citation

Ghotra, V. P. S. (2013, December 19). *Identification of novel targets in prostate cancer progression*. Retrieved from https://hdl.handle.net/1887/22947

Version:	Corrected Publisher's Version
License:	Licence agreement concerning inclusion of doctoral thesis in the Institutional Repository of the University of Leiden
Downloaded from:	https://hdl.handle.net/1887/22947

Note: To cite this publication please use the final published version (if applicable).

Cover Page

Universiteit Leiden

The handle http://hdl.handle.net/1887/22947 holds various files of this Leiden University dissertation

Author: Ghotra, Veerander Paul Singh
Title: Identification of novel targets in prostate cancer progression
Issue Date: 2013-12-19

CHAPTER 2

AUTOMATED MICROINJECTION OF CELL POLYMER SUSPENSIONS IN 3D ECM SCAFFOLDS FOR HIGH-THROUGHPUT QUANTITATIVE CANCER INVASION SCREENS

Hoa H Truong[1], Jan de Sonneville[2], Veerander PS Ghotra[1], Jiangling Xiong[1], Leo Price[1], Pancras Hogendoorn[3], Herman Spaink[4], Bob van de Water[1],Erik HJ Danen[1]

Published in Biomaterials,2012 Jan;33(1):181-8

[1]Division of Toxicology, Leiden Academic Center for Drug Research, Leiden University, Einsteinweg 55,2333 CC, Leiden,The Netherlands;[2]Division of Biophysical Structural Chemistry, Leiden Institute of Chemistry, Leiden University, Einsteinweg 55, 2333 CC Leiden, the Netherlands;[3]Department of Pathology, Leiden University Medical Center, Albinusdreef 2, 2333 ZA, Leiden, The Netherlands; [4]Institute of Biology, Leiden University

ABSTRACT

Cell spheroids (CS) embedded in 3D extracellular matrix (ECM) serve as in vitro mimics for multicellular structures in vivo. Such cultures, started either from spontaneous cell aggregates or single cells dispersed in a gel are time consuming, applicable to restricted cell types only, prone to high variation, and do not allow CS formation with defined spatial distribution required for high-throughput imaging. Here, we describe a novel method where cell-polymer suspensions are microinjected as droplets into collagen gels and CS formation occurs within hours for a broad range of cell types. We have automated this method to produce CS arrays in fixed patterns with defined x-y-z spatial coordinates in 96 well plates and applied automated imaging and image analysis algorithms. Low intra- and inter-well variation of initial CS size and CS expansion indicates excellent reproducibility. Distinct cell migration patterns, including cohesive strand-like- and individual cell migration can be visualized and manipulated. A proof-of-principle chemical screen is performed identifying compounds that affect cancer cell invasion/migration. Finally, we demonstrate applicability to freshly isolated mouse and human tumor biopsy material - indicating potential for development of personalized cancer treatment strategies.

INTRODUCTION

Cells grown under classical 2D culture conditions behave differently from the same cell types grown in vivo. In addition to soluble factors produced in the in-vivo microenvironment, differences in cell shape, intercellular contacts, and connections to ECM have striking effects on gene expression, cell survival, proliferation, differentiation, cytoarchitecture, and migration. Various systems have been developed to culture cells within 3D ECM environments, aimed at more closely mimicking the in-vivo context (1,2). Several of these systems produce 3D cell aggregates in which, after compaction, depletion of oxygen, nutrients, and growth factors occurs in the core, leading to cell heterogeneity depending on the position in the resulting CS (3,4). Multistep methods are used in which aggregates are allowed to form spontaneously and, following a compaction phase, can subsequently be transferred to a 3D ECM. The best-known example of this approach is the “hanging drop assay” that was developed to create embryoid bodies from ES cells and has also been applied to cancer cell lines to produce tumor-like structures (5,6). Alternative methods involve mixing of single cell suspensions with a solidifying ECM, resulting in individual cells that eventually form spheroids randomly within a 3D ECM structure (7), or seeding polymeric scaffolds with cell/ECM suspensions (2). Cell behavior in 3D cultures is controlled by chemical (composition) and physical (rigidity, cross-linking) properties of the gel. Natural ECM proteins can be used such as collagen, fibrinogen, or the laminin-rich matrigel to represent the in-vivo ECM composition most relevant to a given cell type. More recently, synthetic polymers have been developed for 3D CS culture environments although it remains to be established how well these support a variety of cell behavioral outputs, including cell migration (8). Collagen type 1 is an abundant polymer in ECM in vivo, and it is widely used for 3D cultures. Various physical properties of the collagen gel, such as rigidity and pore size modulate stem cell differentiation, cancer growth, and cell migration (9-11). Cells can use various migration strategies in 3D environments, including mesenchymal or amoeboid individual cell migration modes or collective invasion strategies, depending on properties of the cells and of the matrix (10). Changes in matrix pore size can force cells to adopt alternative migration strategies or - if too extreme - pose a barrier to cell migration. Importantly, cells can modify the ECM by physical deformation and proteoly-

sis, to overcome such barriers (12). Chemical compound screens as well as RNAi screens for various types of cellular functions, including survival, growth, differentiation, and migration are mostly performed in 2D culture conditions. Methods to analyze cells in 3D based on the hanging-drop assay are labor and time intensive; are limited to cell types that are cohesive and aggregate spontaneously; and are prone to high variability between experiments due to variation in aggregation and compaction time and CS size. Alternative methods in which single cell suspensions are mixed with soluble ECM substrates that are subsequently allowed to form a gel are relatively easy to perform but also have several major disadvantages: formation of CS depends on the ability of a cell type to survive and proliferate as single cells in low adhesion conditions for extended periods; CS formation is time consuming; CS show a large variation in size; and CS form at random locations, which is disadvantageous for imaging purposes. To allow for CS formation that is relatively fast and easy, highly reproducible, and overcomes the disadvantages described above we have developed a novel method where cell-polymer suspensions are microinjected into multiwell plates containing a collagen gel. This method has been automated to produce CS arrays with highly reproducible properties in large quantities in 96 well plates. We use this system to visualize distinct 3D migration strategies and regulation of those strategies by ECM properties and actomyosin contractility. We demonstrate applicability in high-throughput screening platforms in a chemical screen for compounds that affect breast cancer invasion/migration. Finally, we apply the method to cell suspensions derived from fresh tumor biopsies, which opens the possibility to test therapeutic strategies on freshly isolated material from individual patients.

RESULTS

Development and characterization of the method

To design a protocol that rapidly produces CS with highly reproducible characteristics, we developed a novel method based on microinjection. For the microinjection method we mixed cells with polyvinylpyrrolidone (PVP), which is an inert (hydrophilic) water-soluble synthetic polymer, also used as emulsifier, food-additive (E1201) and as solubilizing agent for injections (13). In our application it was used to delay cell sedimentation within the capillary needle. Furthermore, in our experience cells rapidly disperse in the absence of PVP while cells injected in the presence of PVP remained localized (e.g. trapped by the polymer) at the site of injection, allowing time for aggregation and CS formation. We first compared our method to the established hanging drop assay (5). Twenty µl drops containing $5x10^3$ GEß1 cells were used to create hanging drops in an inverted 10 cm dish (Fig. 1a). The time required to form cell aggregates was 24h. These cell aggregates were transferred to agarose-coated dishes where they formed tightly packed spheroids over a period of 48h. Next, the spheroids were embedded in 2.4 mg/mL collagen solution that was subsequently allowed to solidify. For microinjection, GEß1 cells were suspended in 2% PVP, loaded into a pulled glass needle, and ~80nL droplets containing ~$1x10^4$ cells were injected directly into preformed 2.4 mg/mL collagen gels where they formed tightly packed spheroids within 1h (Fig. 1a). Microinjection-derived CS at 24h post-injection and hanging-drop-derived CS at 96h post initiation (24h in collagen) displayed similar cell migration the following days (Fig. 1b). Microinjection-derived CS were also established from 4T1 mouse breast carcinoma cells where E-cadherin staining marked cell-cell contacts within the first day post-injection that were maintained for at least 96h (Fig. 1c). CS derived by microinjection of different cancer- or non-cancerous cell types allowed analysis of various distinct motile strategies in 3D (Fig.1d). Cell types that do not typically form cell-

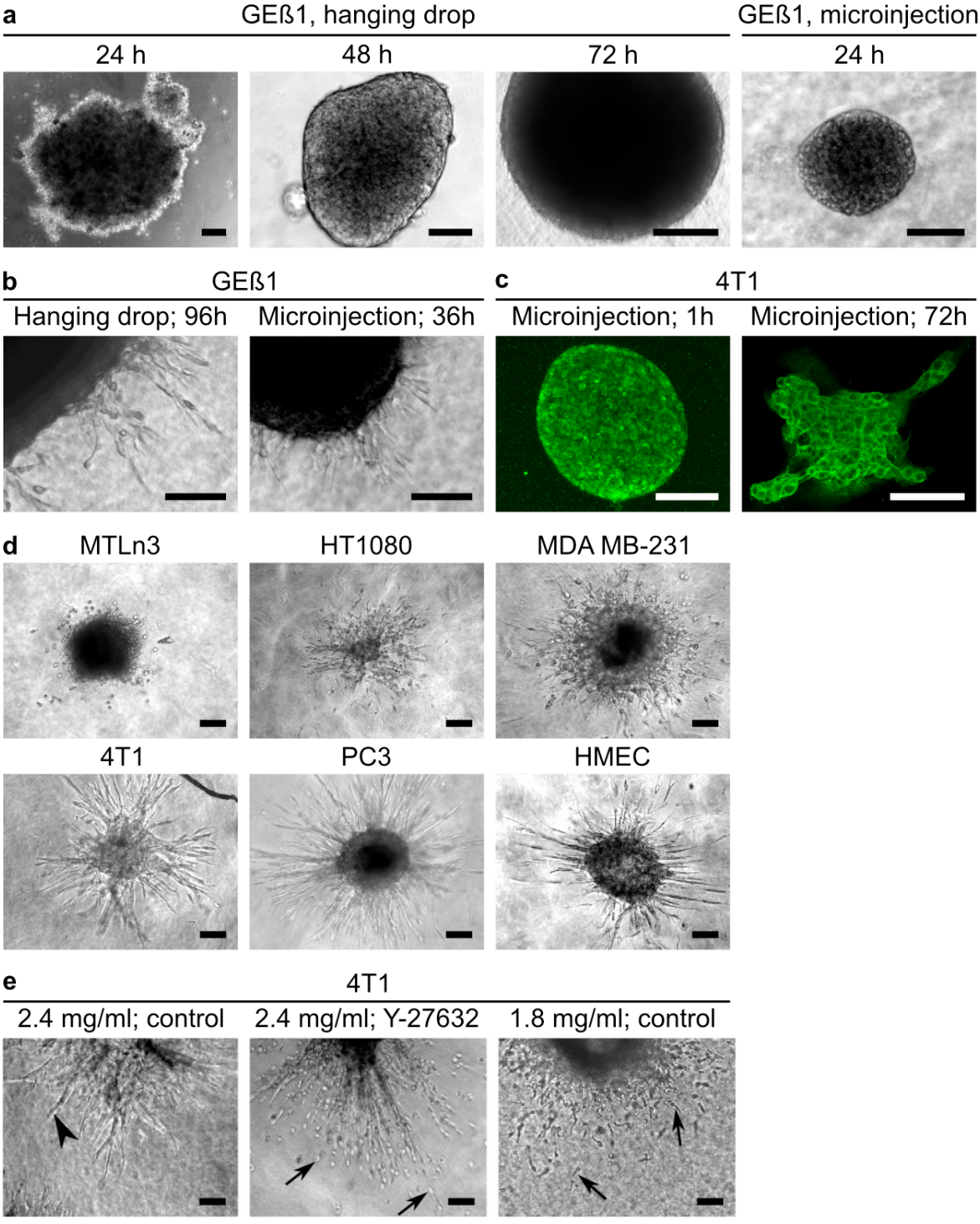

FIGURE 1.*Characteristics of microinjection-derived spheroids.* A, Comparison of hanging-drop and microinjection method for GEß1 cells. B, Migration of GEß1 cells from hanging-drop and microinjection-derived spheroids. C, E-cadherin staining in spheroids at indicated timepoints post-injection for 4T1 cells. D, Different modes of cell migration from spheroids for indicated cell types showing individual (top row) and cohesive strand migration (bottom row). E, Modulation of cell migration modes by alterations in collagen gel network (left and middle) or interfering with cytoskeletal network (right image, ROCK inhibitor). Arrowheads indicate cohesive migration strands; arrows indicate individual migrating cells. Scales, 120 µm.

cell contacts in 2D cell culture (and that are typically difficult to study in 3D using the hanging-drop-, liquid overlay-, or other assays in absence of additives like matrigel (14,15) such as MTLn3 and MDA-MB-231 breast cancer cells and HT1080 fibrosarcoma cells, displayed amoeboid (MTLn3)or mesenchymal (HT1080 and MDA-MB-231) movement of individual cells. On the other hand, 4T1 breast cancer, and human microvascular endothelial cells (HMEC) that grow as islands in 2D culture, invaded as cohesive strands into the collagen matrix.ECM rigidity influences cell behavior in 3D and the actin cytoskeleton is believed to be essential for sensing and responding to such physical ECM properties (12). We used these CS to study the effect of alterations in ECM network composition or intracellular cytoskeletal network properties on migration strategies in 3D. Lowering ECM rigidity by decreasing collagen concentration from 2.5 to 0.25 mg/mL or lowering cytoskeletal tension by application of a ROCK inhibitor, both caused a switch from cohesive strand invasion to individual cell migration in 4T1 cells (Fig. 1e). This suggests that tension exerted on cell-cell adhesion structures either from outside or inside the cell is required for cohesive 3D movement. Altogether, these results demonstrate that the microinjection method produces CS for 3D growth and migration studies rapidly (hours versus days), conveniently (one step), with a broad spectrum of cell types including those that are incompatible with previous methods, and displaying a variety of migration patterns.

Method automation

Since this method has the potential to rapidly create CS with high reproducibility for large- scale analysis in 3D ECM of cell growth and migration/invasion we set up a procedure to automate the CS formation process. For this purpose, a 96 well plate containing 60 µL collagen gel per well was placed on a motorized stage and the glass needle containing the cell/PVP suspension described above was placed vertically in a motorized micromanipulator above the stage (Fig. 2a). After calibration of needle and 96-well plate using camera vision from under the stage, a computer script was used to automate the injection process with various macros.With this set up, cell droplets were injected resulting in spheroids of ~300 µm diameter (Movie S1). To increase reproducibility, using commercial needles reduced needle tip diameter variance and gels were prepared from a single large batch of collagen isolated in-house from rat-tail. Various layouts of injection patterns were tested. A hexagonal pattern of 19 spheroids spaced at 1.2 mm started to show interaction between migration strands of CS at day 4 but a less dense hexagon pattern of 7 spheroids at 2 mm spacing provided sufficient spacing for 96h analysis of CS migration (Fig. 2b,c). Visual inspection indicated reduced CS migration on the most outer rows and columns of each plate, pointing to edge effects. We therefore chose to exclude these wells in all further experiments. We determined reproducibility in all other wells and detected no significant intra- or inter-well variation in initial CS size (ANOVA, $P>0.5$) or CS expansion over ~92h (ANOVA, $P>0.5$) (Fig.2d). These data demonstrate that the microinjection method can be automated to create with high reproducibility and predefined x-y-z coordinates CS arrays in 96 well plates. Such properties make this protocol ideal for automated imaging strategies.

Application of the method to automated drug screens

A proof of principle drug screen was performed to test the applicability of this procedure to automated high-throughput drug screening assays (HTS). 4T1 CS were generated and various previously described inhibitors, including AG1478 (EGFR), PP2 (Src), ML-7 (MLCK), Y-27632 (ROCK), NSC23766 (Rac), SB-431542 (TGFβR activin-like kinases), AG-82 (EGFR), LY-294002 (PI3K), JSI-124 (STAT3) were added one hour later

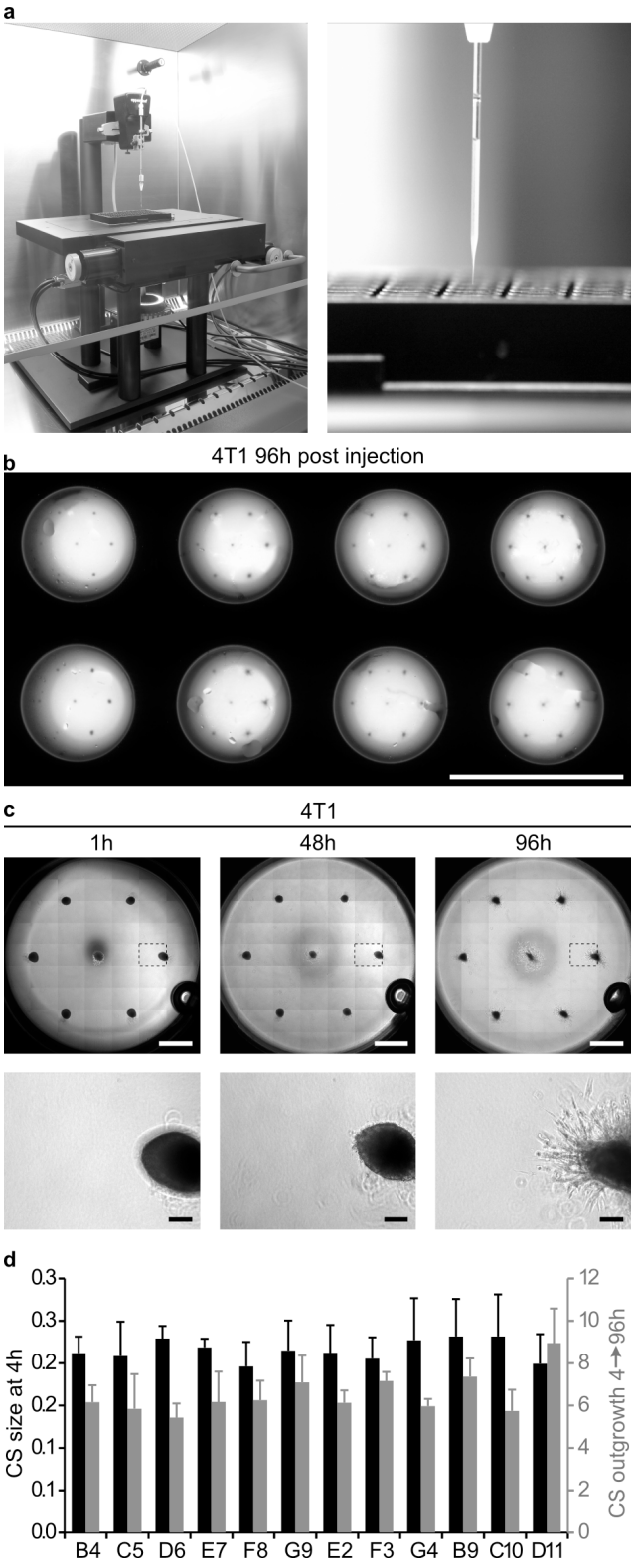

FIGURE 2. *Automated production of spheroid arrays*. A, Automated injection system (left) and cell/PVP suspension in needle during injection (right). B, Bottom view of multiple wells with 4T1 spheroid arrays 96 hours post-injection. Scale, 10mm. C, Upper row shows stitched brightfield images showing spheroid arrays at indicated timepoints. Scale, 1 mm. Bottom row shows cell migration from single bright-field images of spheroids marked by dashed rectangle in upper row. Scale, 100 µm. D, Mean and SD for initial spheroid size 4h post-injection (black bars) and CS migration over ~4 days determined from outline of migration strands (grey bars) obtained from all 7 spheroids /well for indicated wells of a 96-well plate.

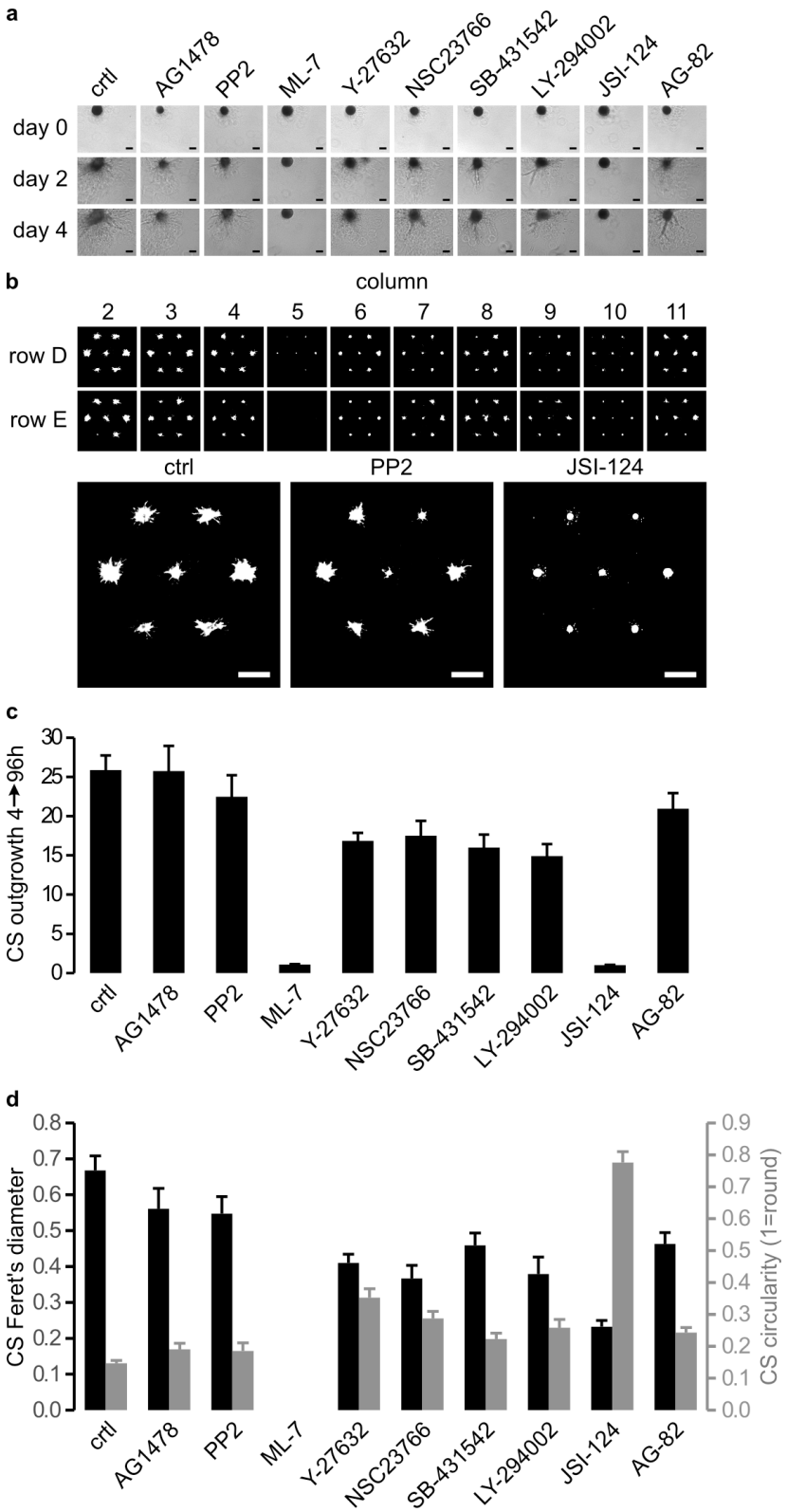

FIGURE 3. *Results from a drug screen performed on 4T1 cells in a 96 well plate.* A, DIC images showing tumor cell migration in the presence of indicated inhibitors at indicated timepoints (scale = 100 µm). B, Top 2 rows, rhodamine-phalloidin staining and thresholding for indicated wells at 4 dpi (columns correspond to treatments from A; rows represent duplicates); bottom row, zoom in on well D2 (Ctr), D4 (PP2), and D10 (JSI-124). Scale, 1 mm. C, effect of indicated inhibitors on CS migration over ~4 days determined from outline of migration strands derived from DIC images in A (mean and SD for 14 spheroids derived from 2 wells is shown). D, Quantification of data derived from automated analysis of fluorescent images shown in B (mean and SD for 14 spheroids derived from 2 wells is shown).

at different concentrations (4, 10, 20 μM) in duplicate. Effects on cell migration could be clearly observed by DIC imaging after 2 and 4 days for ML-7 and JSI-124 (Fig.3a). For automated imaging and image analysis protocols, we labeled the actin cytoskeleton at day 4 of all 10 μM treatments and controls (Fig.3b). This allowed automated capture of Z-stacks that were converted to maximum projection images, thresholded, and used for automated multiparameter analysis including Feret's diameter and circularity. Visual inspection and manual assessment of Feret's diameter from DIC images at day 0 and 4 demonstrated that initial CS size, CS expansion, and inhibition of invasion by ML-7 and JSI-124 were highly reproducible (Fig. 3a,c). Automated image analysis fitted well with these data showing that ML-7 and JSI-124 caused significantly reduced Feret's diameters ($p<0.05$) (Fig.3d). For JSI-124 this correlated with increased circularity ($p<0.05$) in agreement with inhibition of invasion and a remaining round CS. The extremely low values observed for ML-7 (Fig. 3d) despite the fact that a CS was observed by DIC (Fig.3a) can be explained by ML-7-induced loss of filamentous actin fibers causing reduced staining in this particular method. Alternative staining procedures should lead to improvement and compatibility with real-time analysis. Nevertheless, the reproducibility of the injection procedure (Fig. 2 and 3) combined with the similarity between visual inspection and automated imaging (Fig. 3c,d), demonstrates that this automated injection system can be coupled to fully automated imaging and image analysis methodology that is accurate and reproducible.

Compatibility of the method with primary biopsy material

We determined if this methodology is compatible with freshly isolated biopsy material. First, a cell suspension was generated from 4T1-GFP orthotopic breast tumors in mice using collagenase- treatment. In contrast to alternative methods, the microinjection method circumvents any 2D tissue culture steps, which may cause altered cell behavior (16-20). Following injection, these cells rapidly formed CS from which migration was analyzed after 3 days (Fig. 4a). CS were stained for actin and DNA and the near complete overlap between actin and GFP staining demonstrates that these CS consist mainly of tumor cells. Next, cell suspensions were derived by collagenase treatment of freshly isolated human osteosarcoma and chondrosarcoma tissue. Following injection, CS readily formed from these human biopsies and survival and migration could be studied for up to one week with the two tumor types showing distinct migratory behavior (Fig.4b). Osteosarcoma mainly displayed individual amoeboid movement whereas chondrosarcoma showed predominantly individual mesenchymal movement. We treated these CS with the range of compounds described above at 10 μM starting one day post-injection. Several of the chemical inhibitors effectively inhibited migration of both tumor types (Fig. 4b,c). Notably, the ROCK inhibitor Y-27632 did not affect mesenchymal movement but caused switching from amoeboid to mesenchymal movement in the osteosarcoma cells, in line with the described requirement for ROCK activity only in amoeboid single cell movement (21). Taken together, these data indicate that the automated CS injection methodology has the potential to be used for drug testing on tumor cells freshly isolated from individual patients.

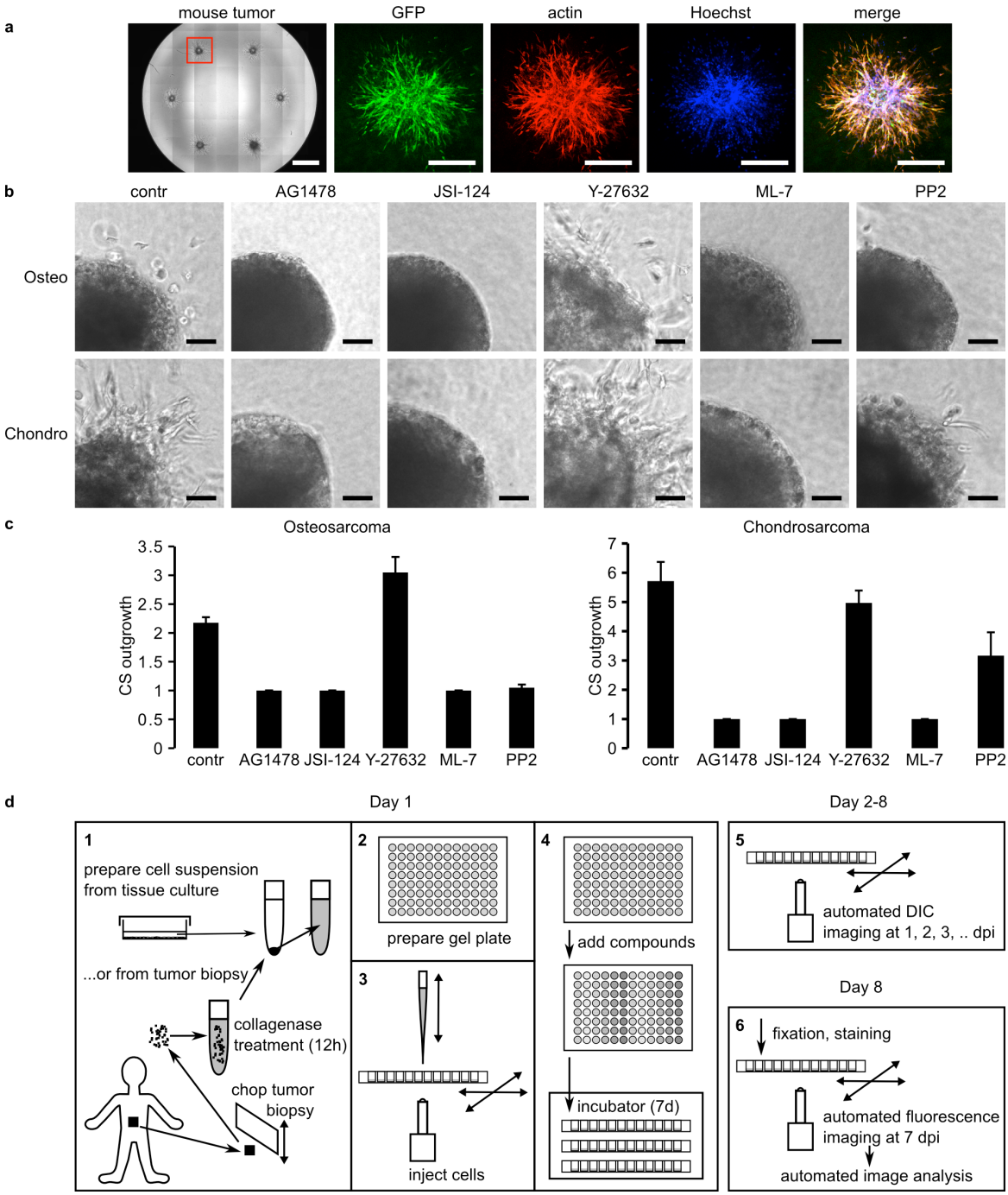

FIGURE 4. *Application to tumor biopsies*. A, Overview DIC image (left) and zoom in on individual spheroid obtained from 4T1-GFP orthotopic mouse breast tumor. Scales, 1 mm (left DIC); 500µm (fluorescent images). B, DIC images showing spheroids derived from osteosarcoma (top) and chondrosarcoma biopsy (bottom) treated with indicated inhibitors. Scale, 100µm. C, effect of indicated inhibitors on CS migration over ~4 days determined from outline of migration strands derived for DIC images in A (mean and SD 12 spheroids derived from 2 wells is shown). D, Schematic overview of high-throughput spheroid screening indicating procedure at day 1 (steps 1-3) and imaging in absence or presence of compounds at days 2-8 (steps 4-6).

DISCUSSION

Here, we describe a method for generation of 3D CS cultures based on microinjection of cell suspensions into premade gels, that has a number of features making it highly useful for drug screening applications: compared to previous methods it is easy (one step procedure) and fast (minutes instead of days); CS are generated with high accuracy at predetermined x-y-z positions in multiwell plates; it is applicable to many different cell types irrespective of the ability of cells to form spontaneous cell-cell contacts; it shows good intra- and inter-well reproducibility with respect to CS size and migration; because of the predefined coordinates of each individual CS the method can easily be combined with fully automated imaging and image analysis protocols (Fig. 5.4d). 2D culture conditions are a very poor representation of the environment cells encounter in vivo. Besides implications for cell biology studies, this has important consequences for the interpretation of genetic - and drug screens (22). So far, these have mostly been performed on 2D cultures. For the study of tumor cell invasion the Boyden chamber assay (trans-well migration assay) is also commonly used. Here, a monolayer of cells migrates through a thin layer of gel to reach the bottom of a filter. This particular assay does not resemble cells disassociating from a solid tumor. For this purpose, CS cultures have been developed that provide a pathophysiological context that mimics solid cancer microenvironments. However, these have not been used for large-scale drug screens due to the complicated procedures, which negatively affect reproducibility of results and lead to higher costs. Reproducibility of CS size is critical for a reliable 3D culture platform. Size and compactness of CS will inevitably affect drug penetration and previous studies have indicated that CS with diameters between 200 and 500µm are required to develop chemical gradients (e.g. of oxygen, nutrients, and catabolites) that may represent conditions found in tumors (3,4,23 - 26). Our automated approach yields spheroids with a diameter of ~300µm, a size that may thus represents solid tumor traits.We have used collagen-based gels but the same method could be easily adapted to studies using alternative 3D matrices. The type and concentration of matrix proteins will have considerable influence on scaffold structure, rigidity, and porosity, which will impact on cell morphology, survival, proliferation, and migration efficiency (8,27,28). We find that changing collagen concentrations has a major impact on CS cell migration and that optimal conditions differ for distinct cell types, in agreement with findings from others (8,27-30). Hence, it is essential that gel formation is standardized and optimized for each cell type. The use of ECM proteins such as collagen has some limitation in terms of controlling batch-to batch variation. Therefore, stabilization by chemical cross-linking may be applied to better control mechanical properties as porosity and mechanical strength. A number of different cross-linking agents that react with specific amino acid residues on the collagen molecule, synthetic biopolymer scaffolds, and self-assembling synthetic oligopeptide gels are available to address this (27,28,31,32). We demonstrate that we can automate each step of the procedure, from injection of cell suspensions to imaging and image analysis, while maintaining reproducibility. Our method not only accelerates and simplifies CS formation but by generating up to 7 CS per well at predefined x-y-z coordinates it is compatible with fully automated imaging procedures, enhanced data collection, and robust statistical analysis. We present a small drug screen to demonstrate such properties. Finally, we show that the method presented here can be used for CS formation directly from freshly isolated tumor biopsy material without the need of any intermediate culture steps. This eliminates artificial traits induced by 2D culture. A fully analyzed CS cancer migration screen in 96 well plates can be derived from a biopsy within 1 week. This opens the door to screening on a patient-by-patient basis for drug sensitivity of tumor cells under conditions that may closely mimic the in-vivo pathophysiological situation. Clinical tests to validate inhibi-

tor effects in CS screens by comparing with therapeutic efficacy can be performed without further modifications of the presented system. Moreover, expansions of this method can be envisioned in which multiple cell types are combined (e.g. cancer cells and cancer-associated fibroblasts and/or endothelial cells) to further improve representation of the complex tumor microenvironment.

MATERIALS AND METHODS

Cell culture

The following cell lines were obtained from ATCC: MDA-MB-231, MTLn3, PC-3, HT1080, 4T1, and MAE. GEβ1 was described earlier(33). All cell lines were cultured under standard cell culture conditions indicated by ATCC or as described (33) at 37.C, 5% CO2 in a humidified incubator. Primary mouse tumor cell suspensions were derived from surplus mouse breast tumor material by mincing using scalpel and tissue chopper followed by 2-hour collagenase treatment at 37 degree celsius. Human biopsy material was obtained from surplus material from patients that were surgically treated for chondrosarcoma or osteosarcoma. Tumor cell suspensions were derived from biopsies by 12h collagenase treatment at 37.C. All human specimens were handled in an anonymized coded fashion according to the National ethical guidelines for secondary use of patient-derived material.

Preparation of collagen

Collagen type I solution was obtained from Upstate-Milipore or isolated from rat-tail collagen by acid extraction as described previously (34). Collagen was diluted to indicated working concentrations of ~2.4 mg/mL in PBS containing 1xDMEM (stock 10x, Gibco), 44 mM NaHCO3 (stock 440 mM, Merck), 0.1 M Hepes (stock 1M, BioSolve).

Hanging drop method

~ 5000 cells in 20 µL droplets were dispensed onto a 10 cm dish that was inverted over a dish containing 10 mL DMEM. After 24h, cell aggregates were harvested using a Pasteur pipette and transferred into 10 cm dishes coated with 0.75% agarose submerged in 10mL DMEM. After 48h, spheroids had formed and these were embedded into a 2.4 mg/mL collagen solution using a Pasteur pipette. Collagen gels were allowed to solidify at 37.C for 30 min and overlaid with DMEM. Cell invasion was recorded for 3 days using an inverted phase contrast light microscope (Nikon Eclipse E600).

Cell preparation for injection method

Cell suspensions derived from trypsin-detached adherent cultures or from collagenase - treated biopsies were filtered to remove clumps, centrifuged at 1000 rpm for 5 minutes, and washed twice with PBS. ~$7x10^6$ cells were re-suspended in 30 µL PBS containing 2% polyvinylpyrrolidone (PVP; Sigma-Aldrich). The PVP/cell suspension was loaded into a beveled pulled glass needle (Eppendorf CustomTip Type III, OD [µm] 60, Front surface 40, Flexibility: rigid).

Manual injection

Cell suspensions in 2% PVP were microinjected (~1x10^4 cells/droplet) with a microinjector (20 psi, PV820 Pneumatic PicoPump, World Precision Instruments, Inc) into solidified collagen gels in 8 well μslides (IBIDI).

Automated injections

A glass-bottom 96 well plate (Greiner) containing 60 μL solidified 2.4 mg/ mL collagen gel per well was placed in a motorized stage (MTmot 200x100 MR, Marzhauser) connected to a controller (Tango, Marzhauser). A motorized micro-manipulator (Injectman II, Eppendorf) was positioned above the stage and connected to a pump (Femtojet Express, Eppendorf) featuring an external compressor (lubricated compressor, model 3-4, JUN-AIR). A firewire camera (DFK41BF02.H, The Imaging Source) equipped with an 8x macro lens (MR8/O, The Imaging Source) was placed beneath the stage for calibration and imaging. All components were connected to the controlling computer (Ubuntu AMD64).

A multi-threaded control program was written in Python using PySerial and wxPython. Coriander software (http://damien.douxchamps.net/ieee1394/coriander) was used for imaging.After the program was calibrated for the 96 well plate the camera height was adjusted to focus on the bottom of the 96 well plate. The plate was then removed for needle calibration: the injection needle was fixed in the Injectman and moved, using the Injectman controller, into the center of the image. The injection height was set to 200μm above the bottom of the (virtual) plate. After the needle was moved up, the plate was placed back in position and the upper left well was used for multiple test injections to adjust pump pressure and injection time for optimization of the droplet size (~8nL ~ 300μm diameter) using video inspection. Subsequently, using a pre-defined macro defining x-y coordinates and number of injections per well, all wells were injected with the same pressure and injection time.

Microscopy and image analysis

Manually injected CS were monitored daily using a Nikon Eclipse E600 microscope. CS generated by automated injection were used for montage imaging using a Nikon TE2000 confocal microscope equipped with a Prior stage controlled by NIS Element Software and a temperature and CO2-controlled incubator. Differential interference contrast (DIC) images were captured using a charged coupled device (CCD) camera with NIS software at 10x dry objective. Quantification of CS invasion area was analyzed from DIC images using ImageJ. The CS ellipsoidal area after three days was estimated using the diameter in x and y axis (pi*radius-x*radius-y) occupied by cells in the 10x montage image in the mid-plane of each spheroid and normalizing to the occupied area 1h after injection. One-way ANOVA was performed to test the significance of the data. The data are presented and plotted as average and standard error of the mean. For automated imaging, wells containing gel-embedded spheroids were treated with a fixation and staining cocktail containing 3.7% paraformaldehyde, 0.2% Triton X-100 (Sigma) and 0.1 μM rhodamine Phalloidin (Sigma) for 3 hrs. Wells were washed extensively with PBS and plates were imaged on a Becton Dickinson Pathway 855 using a 4X lens. A montage of 12 frames was made for each Z plane, with a total of 24 Z planes at an interval of 50 μm. Image stacks were converted into 2D maximum fluorescence intensity projections using ImagePro 7.0. CS were then digitally segmented using ImageJ to identify the outline of individual CS and multiple parameters were measured, including Feret's diameter, roundness, and number of CS scored in each well. For immu-

nostaining of E-cadherin, gels were incubated for 30 mins with 5 µg/ mL collagenase (Clostridium histolyticum, Boehringer Mannheim) at room temperature, fixed with 4% paraformaldehyde, permeabilized in 0.2% Triton X-100, and blocked with 10% FBS. Gels were incubated with E-cadherin antibody (BD Transduction Laboratories) overnight at 4 degree celsius followed by Alexa 488-conjugated secondary antibody (Molecular Probes/Invitrogen) for 2 hrs at room temperature and Hoechst 33258 nuclear staining (Molecular Probes/Invitrogen) for 30 min at room temperature. Preparations were mounted in Aqua-Poly/Mount solution (Polysciences, Inc) and analyzed using a Nikon TE2000 confocal microscope. Z-stacks (~100 stacks, step of 1 µm) were obtained using a 20x dry objective, imported into ImageJ, and collapsed using extended depth of field plugin (Z projection) into a focused composite image.

Drug Treatment

LY-294002 (phosphatidylinositol 3-kinase), JSI-124-cucurbitacin (STAT3/Jak2), NSC23766 (Rac1), and AG-82 (general protein tyrosine kinases) were purchased from Merck/CalBiochem. PP2 (Src) and ML-7 (MLC kinase) were purchased from ENZO. Y-27632 (Rock), SB-431542 (TGFβ) and AG1478 (EGFR) were purchased from BioMol Tocris. Cell migration was analyzed in the absence and presence of inhibitors for 4 days.

ACKNOWLEDGMENTS

We thank ZF-screens B.V. (Leiden, NL) for permitted use of the microinjectorsystem, which was modified for this project, with the technical help of Fred Schenkel and Ewie de Kuyper (Department of Fine Mechanics). We thank Wies van Roosmalen and Sylvia le D.v.dec for mouse tumor biopsy material. We acknowledge financial support from the Netherlands Organization for Science (NWO; Cyttron project), the Dutch Cancer Society (project UL-2006- 3521), and EU FP7 (HEALTH-F2-2008-201439).

REFERENCES

1. Kenny PA, et al. The morphologies of breast cancer cell lines in three-dimensional assays correlate with their profiles of gene expression. Mol Oncol. 1: 84 - 96, (2007).

2. Fischbach C, et al. Engineering tumors with 3D scaffolds. Nat Methods 4: 855 - 860 (2007).

3. Mueller-Klieser W. Multicellular spheroids. J Cancer Res Clin Oncol 113: 101 - 122 (1987).

4. Sutherland RM. Cell and environment interactions in tumor microregions: the multicell spheroid model. Science, 240: 177 - 184 (1988).

5. Keller GM. In vitro differentiation of embryonic stem cells. Curr Opin Cell Biol, 7: 862 - 869 (1995).

6. Kelm JM, Timmins NE, Brown CJ, Fussenegger M & Nielsen LK. Method for generation of homogeneous multicellular tumor spheroids applicable to a wide variety of cell types. Biotechnol Bioeng, 83: 173 - 180 (2003).

7. Lee GY, Kenny PA, Lee EH & Bissell MJ. Three-dimensional culture models of normal and malignant breast epithelial cells. Nat Methods, 4: 359 - 365 (2007).

8. Loessner D, et al. Bioengineered 3D platform to explore cell-ECM interactions and drug resistance of epithelial ovarian cancer cells. Biomaterials 31: 8494 - 8506 (2010).

9. Buxboim A & Discher DE. Stem cells feel the difference. Nat Methods, 7: 695 - 697 (2010).

10. Friedl P & Wolf K. Plasticity of cell migration: a multiscale tuning model. J Cell Biol, 188: 11 - 19 (2010)

11. Levental KR, et al. Matrix crosslinking forces tumor progression by enhancing integrin signaling. Cell, 39: 891 - 906 (2009).

12. Lammermann T & Sixt M. Mechanical modes of ‘amoeboid’ cell migration. Curr Opin Cell Biol, 21: 636 - 644 (2009).

13. Haaf F, Sanner A & Straub F. Polymers of N-Vinylpyrrolidone: Synthesis, Characterization and Uses. Polymer J, 17: 143 - 152 (1985).

14. Ivascu A & Kubbies M. Rapid generation of single-tumor spheroids for high-throughput cell function and toxicity analysis. J Biomol Screen, 11: 922 - 932 (2006).

15. Ivascu A & Kubbies M. Diversity of cell-mediated adhesion in breast cancer spheroids. Int J Oncol, 31: 1403 - 1413 (2007).

16. Bjerkvig R, Tonnesen A, Laerum OD & Backlund EO. Multicellular tumor spheroids from human gliomas maintained in organ culture. J Neurosurg, 72: 463 - 75 (1990).

17. Bissell, M.J. The differentiated state of normal and malignant cells or how to define a “normal” cell in culture. Int Rev Cytol, 70: 27 - 100 (1981).

18. Walpita D & Hay E. Studying actin-dependent processes in tissue culture. Nat Rev Mol Cell Biol, 3: 137 - 141 (2002).

19. Corcoran A, et al. Evolution of the brain tumor spheroid model: transcending current model limitations. Acta Neurochir, 145: 819 - 824 (2003).

20. Beliveau A, et al. Raf-induced MMP9 disrupts tissue architecture of human breast cells in three dimensional culture and is necessary for tumor growth in vivo. Genes Dev, 15: 2800 - 2811 (2010).

21. Sahai E & Marshall CJ. Differing modes of tumor cell invasion have distinct requirements for Rho/ROCK signalling and extracellular proteolysis. Nat Cell Biol, 5: 711 - 719 (2003).

22. Pampaloni F, Reynaud EG & Stelzer EH. The third dimension bridges the gap between cell culture and live tissue. Nat Rev Mol Cell Biol, 10: 839 - 45 (2007).

23. Friedrich J, Ebner R & Kunz-Schughart LA. Experimental anti-tumor therapy in 3-D: spheroids--old hat or new challenge? Int J Radiat Biol, 83: 849 - 871 (2007).

24. Kunz-Schughart LA, Freyer JP, Hofstaedter F & Ebner R. The use of 3-D cultures for high-throughput screening: the multicellular spheroid model. J Biomol Screen, 9: 273 - 285 (2004).

25. Mueller-Klieser,W. Three-dimensional cell cultures: from molecular mechanisms to clinical applications. Am J Physiol, 273: C1109 - 1123 (1997).

26. Mueller-Klieser,W. Tumor biology and experimental therapeutics. Crit Rev Oncol Hematol, 36: 123 - 139 (2000).

27. Bott K, et al. The effect of matrix characteristics on fibroblast proliferation in 3D gels. Biomaterials, 32: 8454 - 8464 (2010).

28. Sung KE, et al. Control of 3-dimensional collagen matrix polymerization for reproducible human mammary fibroblast cell culture in microfluidic devices. Biomaterials, 27: 4833 - 4841 (2009).

29. Cross VL, et al. Dense type I collagen matrices that support cellular remodeling and microfabrication for studies of tumor angiogenesis and vasculogenesis in vitro. Biomaterials, 31: 8596 - 8607 (2010).

30. Zaman MH, et al. Migration of tumor cells in 3D matrices is governed by matrix stiffness along with cell-matrix adhesion and proteolysis. Proc Natl Acad Sci, 103: 10889 - 1089(2006).

31. Rosso F, et al. Smart materials as scaffolds for tissue engineering. J Cell Physiol, 203: 465 - 470 (2005).

32. Peppas, NA, Hilt JZ, Khademhosseini A & Langer R. Hydrogel in Biology and Medicine: From Molecular Principles to Bionanotechnology. Adv. Mater, 18: 1345 - 1360 (2006).

33. Danen EH, Sonneveld P, Brakebusch C, Fassler R & Sonnenberg A. The fibronectin- binding integrins alpha5beta1 and alphavbeta3 differentially modulate RhoA-GTP loading, organization of cell matrix adhesions, and fibronectin fibrillogenesis. J Cell Biol, 159: 1071 - 1086(2002).

34. Rajan N, Habermehl J, Cote M, Doillon CJ, & Mantovani D. Preparation of ready-touse, storable and reconstituted type I collagen from rat-tail tendon for tissue engineering applications. Nat Protocols, 1: 2753 - 2758 (2007).